Universidad del País Vasco Euskal Herriko Unibertsitatea

Facultad de Química
Kimika Fakultatea

Universidad del País Vasco/Euskal Herriko Unibertsitatea

Facultad de Química/Kimika Fakultatea

Grado en Química

TRABAJO FIN DE GRADO

PHOTOINDUCED RAFT POLYMERIZATION FROM NOVEL WATER-SOLUBLE SINGLE-CHAIN NANOREACTORS

Autor: Mikel Iguaran

Dirigido por: José Adolfo Pomposo Alonso y Ester Verde Sesto

Donostia-San Sebastián, July 2022

GIPUZKOAKO CAMPUSA
CAMPUS DE GIPUZKOA
Pº. Manuel de Lardizabal, 3
20018 DONOSTIA-SAN SEBASTIAN
GIPUZKOA

Abstract

Single chain nanoparticles (SCNPs) are ultra-small size nano-objects, which are obtained by the collapse of a single polymer chain. In the literature, there are many examples of potential SCNPs for a range of applications such as biomedicine, catalysis or sensing.[1,2,3] In principle, these nanomaterials could be easily tuned, creating new materials with exceptional properties to be used in novelty applications such as photocatalysis.[4] Only few works describe the use of SCNPs as photocatalyst, being the control of the reaction the most challenging point.

In this project, we described the preparation of new SCNPs with promising properties to be used as photocatalyst in Reversible Addition Fragmentation Chain Transfer (RAFT) polymerization of N-isopropylacrylamide (NIPAM) in water. These photocatalysts, based on SCNPs, were synthesized starting from an amphiphilic copolymer of 2-acetoacetoxy ethyl methacrylate (AEMA, hydrophobic monomer) and oligo(ethylene glycol) methyl ether methacrylate (OEGMA, hydrophilic monomer). Through a post-functionalization of the copolymers, we prepared Iridium-decorated amphiphilic SCNPs (SCNPs-Ir).

In order to have a first evaluation of the photocatalytic performances of SCNPs-Ir, we choose the aqueous photopolymerization of NIPAM as a model reaction. The efficiency of the polymeric photocatalyst was then compared with an unsupported Iridium catalyst, which if employed in the same reaction conditions, led to poor results in terms of mass yield and polydispersity of the final products (Poly(NIPAM), (PNIPAM)).

When using SCNPs-Ir as the photocatalyst, we isolated way better polymerization products (PNIPAMs), in agreement with the typical behaviour of a classical controlled radical polymerization (CRP). In all cases, the products obtained from the photopolymerization reactions were characterized using different experimental techniques, including gel permeation chromatography/size exclusion chromatography (GPC/SEC), dynamic light scattering (DLS) and proton nuclear magnetic resonance (^{1}H NMR).

Resumen

Las nanopartículas poliméricas unimoleculares (NPUs) son nano-objetos blandos de tamaño minúsculo que se obtienen mediante el plegado o colapso de una cadena polimérica. En la literatura, hay muchos ejemplos de NPUs con grandes potenciales para ser utilizados en aplicaciones como la biomedicina, la catálisis o la detección.[1,2,3] Estos nanomateriales podrían ser fácilmente modificados, creando nuevos materiales con propiedades excepcionales para ser utilizados en novedosas aplicaciones como es la fotocatálisis.[4]

En este proyecto, se ha descrito la preparación de nuevas NPUs con propiedades prometedoras para su uso como fotocatalizadores en polimerizaciones de transferencia por adición-fragmentación reversible (RAFT) del N-isopropilacrilamida (NIPAM) en agua. Este fotocatalizador basado NPUs fue sintetizado usando como precursor un copolímero anfifílico sintetizado a partir del 2-acetoacetoxi etil metacrilato (AEMA, monómero hidrofóbico) y oligo(etilenglicol) metil éter metacrilato (OEGMA, monómero hidrofílico). Mediante post-funcionalización de estos copolímeros, preparamos SCNPs anfifílicas decoradas con iridio (SCNPs-Ir).

Para tener una primera evaluación de las actividad fotocataítica de las SCNPs-Ir preparadas, elegimos como reacción modelo la fotopolimerización de NIPAM en agua. La eficacia de este fotocatalizador polimérico se comparó con la del catalizador de iridio sin soportar, el cuál condujo a peores resultados en términos de rendimiento de peso molecular y polidispersidad de los productos finales (Poly(NIPAM), (PNIPAM)).

Al utilizar SCNPs-Ir como fotocatalizador, aislamos productos de polimerización de manera más controlada (PNIPAMs), de acuerdo con el comportamiento típico de una polimerización radical controlada clásica (CRP). En todos los casos, los productos obtenidos de las reacciones de fotopolimerización se caracterizaron mediante diferentes técnicas experimentales, incluyendo la cromatografía de permeación en gel/cromatografía de exclusión de tamaño (GPC/SEC), la dispersión de luz dinámica (DLS) y la resonancia magnética nuclear de protones (^{1}H NMR).

1. Introduction

1.1. Polymers: general features

By definition, polymers are long-chain molecules formed by the covalent union of smaller molecules, or repeating units, called monomers. The process of producing a polymer through a monomer is called polymerization. The number of monomers within the polymer molecule can vary greatly, and the degree to which regularity appears in the order, relative orientation, and the presence of differing monomers within the same polymer molecule can vary as well. Depending on the type of monomers that form a polymer chain, two main type of polymers can be obtained: homopolymers (*e.g.* polyvinyl chloride, PVC) and heteropolymers (*e.g.* acrylonitrile butadiene styrene, ABS and styrene-butadiene-styrene, SBS). The main difference between them is that homopolymers are made from the polymerization of identical monomers whereas heteropolymers are made from the polymerization of two or more different monomers. In particular, copolymers are heteropolymers made from two different monomers. These polymeric materials can be random (the different repetitive units do not follow any pattern), alternating (different monomers are alternatively linked) or block (one monomer complete a sequence and then the other) sequences.[5]

1.2. Classification of polymers

They are lot of ways to classify the polymers, such as depending on their origin, structure, and type of polymerization reaction.[6]

a) Based on origin of source

Polymer are classified depending on their origin in three main groups:

- Natural: these polymers are materials obtained from nature sources (*e.g.* cellulose or proteins).
- Semi-synthetic: they are obtained by modifying natural polymers (*e.g*. cellulose acetate).
- Synthetic: these materials are artificially synthesized polymers (e.g. nylon).

b) Based on structure

As the Figure 1 shows, polymers can be classify depending on their structure as follow:

- Linear polymers: the simplest structures are linear polymers, which are made up of a linear sequence of monomers, obtaining a long straight chain.

- Non-linear polymers: branched and crosslinked polymers are nonlinear polymeric materials: a) branched polymers have branches growing out from the main polymer chain and b) crosslinked polymers are three-dimensional materials where different polymer chains are linked together.

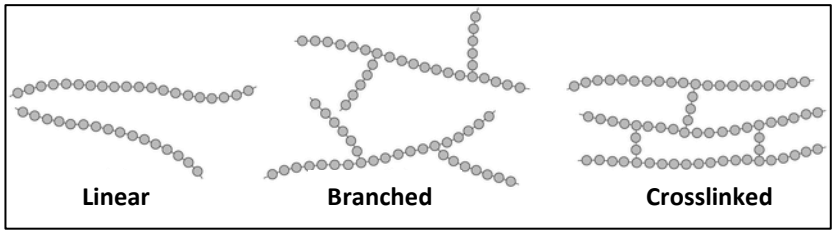

Figure 1: Types of polymers depending on their structure.

c) Based on mode of polymerization

In general terms, there are two basic polymerization reactions to synthetize a polymer: addition polymerization (chain growth polymerization) and condensation polymerization (step growth polymerization).

- Addition polymerization: polymers are formed by the addition of monomers possessing unsaturations. Free radical, ionic and coordination polymerizations are examples of addition polymerizations.
- Condensation polymerization: condensation products are formed by the reaction between a bifunctional or trifunctional monomer unit. In this polymerization a by-product is obtained which usually is water or methanol.

In particular, radical polymerization -Reversible Addition-Fragmentation Chain Transfer (RAFT)- was used to prepare the random copolymer precursor of this project.

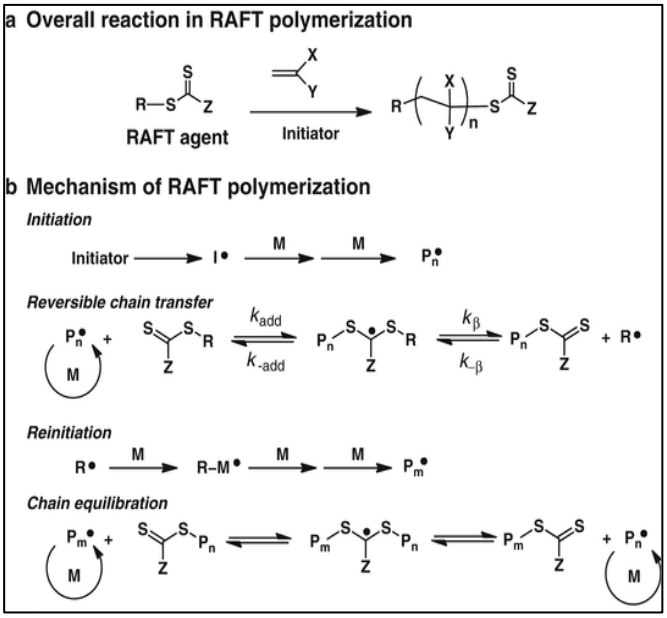

Figure 2: Mechanism of RAFT polymerization.[7]

RAFT is a form of living radical polymerization involving radical polymerization of a monomer in the presence of a chain transfer agent (CTA) (Figure 2). Firstly, the initiator (I) becomes an active specie and reacts with the monomer (M) to create a radical species (Pn•) which is in charge of start the polymerization. The active specie reacts with the CTA/RAFT agent and the R group becomes a reactive species (R•). This reactive specie is capable of re-initiating the polymerization forming a new active chain with another monomer specie (Pm•). Them a new chain equilibration occurs, but in this case the transference agent is attached to the Pn•. The equilibrium between the active chain and the polymer with the CTA, controls the probability of obtaining the same growth for all the molecules. The use of an appropriate RAFT agent and adequate polymerization conditions allows the synthesis of polymers with low dispersity (*Đ*) and defined molecular weight.

1.3. SCNPs: general aspects

Single chain nanoparticles (SCNPs) are small soft nano-objects (<20 nm) prepared by intra-molecular folding/collapse of single polymer chains.[8] Another important characteristic of these polymeric materials is their inherent large surface-to-volume ratio.

1.3.1. SCNPs construction

The molecular weight (M_W) of the precursor polymers of SCNPs and their functionalization degree are essential parameters to control the size of the SCNPs. In addition, the nature of the interactions employed to perform the folding/collapse and the solvent quality (good solvent,

selective solvent) used to prepare SCNPs will also affect the size of the SCNPs. All these parameters will be explained with more details in next sections.

In summary, three main different techniques will allow to synthesize SCNPs (Figure 3):[8]

a. **Controlled polymerization** for the synthesis of the polymer precursors of SCNPs. Through living radical polymerization techniques, the precursor polymer chains can be prepared in a controlled manner in order to obtain nanoparticles with a narrow size distribution.
b. **Polymer functionalization** (if necessary) for the introduction of specific functional groups (reactive groups) into the polymer that allow the folding of the polymer chain.
c. **Intrachain folding/collapse**, which can be generated *via* covalent, non-covalent or dynamic-covalent bonding interactions.

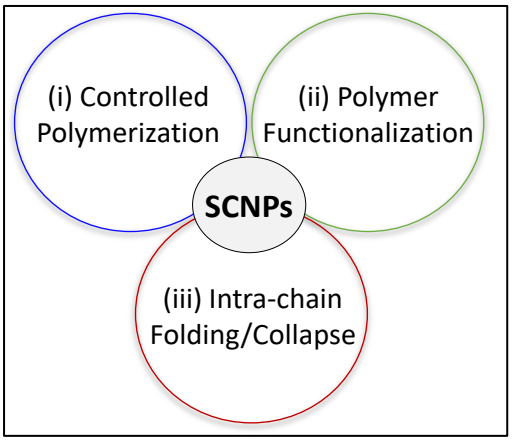

Figure 3: Different techniques involved in the construction of SCNPs.

If we look to the morphology of SCNPs on a solvent, two conformations can be achieved, sparse SCNPs and globular SCNPs (Figure 4), depending on the reaction conditions, the nature of the polymer and the external crosslinker we will obtain one of those morphologies.[9]

Before to describe the main characteristics of sparse and globular SCNPs, a briefly explanation of the difference between good, theta and bad solvent will be introduced:

a. **Good solvent**: interactions between polymer segments and solvent molecules are energetically favourable and will cause polymer coils to expand.[10]
b. **Theta solvent**: is a solvent where polymer coils act like ideal chains assuming a random walk coil conformation.[11]
c. **Bad solvent**: polymer-polymer self-interactions are preferred and the polymer coils will contract.[10]

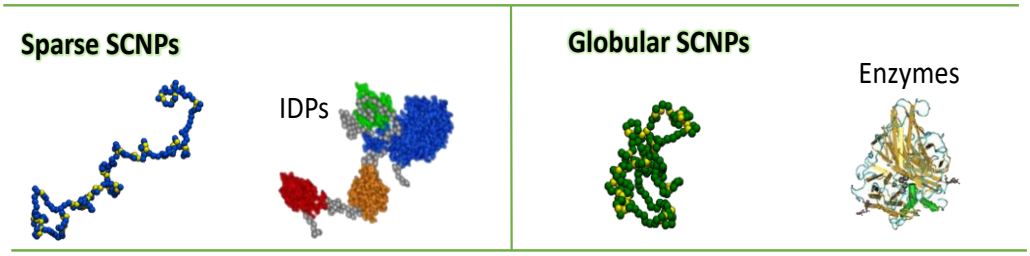

Figure 4: Illustration of sparse and globular morphologies adopted by single chain nanoparticles (SCNPs).

In general, **sparse SCNPs** try to mimic intrinsically disordered proteins (IDPs). These SCNPs are achieved, when we used a good solvent even by the use of highly efficient intra-chain interactions. It should be noted that the conformations exhibited by SCNPs in diluted solutions, synthesized in good solvent conditions, shows many similarities with those displayed by IDPs. Both, SCNPs and IDPs, are intrinsically polydisperse in topology.

Globular SCNPs try to look like enzymes. These SCNPs are obtained from amphiphilic precursors. It should be noted that the core-shell conformation displayed by SCNPs, shows many similarities with those displayed by native proteins. Recently, new approaches of achieving SCNP from neutral and charged amphiphilic copolymer were reported. The potential range of applications of SCNPs have broaden by taking inspiration from the functions of both ordered and disordered proteins.

1.4. Applications

Single chain nanoparticles resulted to be versatile soft nano-systems. As it is recently emerging from the rapid increase in the number of applications in a variety of research fields, such as biomedicine[1], catalysis[2] and sensing[3], just to cite a few, SCNP technology already constitutes a valid platform for a plenty of investigation opportunities.

As mentioned above, the folding of individual polymer chains to functional SCNPs is indeed reminiscent of protein folding to their functional, native state, although current SCNPs lack the perfection in sequence, uniformity in size, and precise morphology that is found in enzymes. Even so, the folding of a synthetic polymer to a collapsed state provides with one (or more) denser local packaging zone(s), which can be exploited not only to enhance catalysis performances, but also to enable catalysis in aqueous media. Their small size (5−10 nm) and ease of functionalization are among the most attractive features that motivate the use of these polymeric architectures.

SCNPs have been employed as highly-efficient nanoreactors in several applications, spanning from the synthesis of gold nanoparticles, ring-opening and controlled radical polymerizations, aldol reactions, aromatic substitutions, to alkynes coupling, only to cite a few.[12-17]

Driven by such promising results obtained with SCNPs, an increasing research activity in this emergent field is expected in the near future.

1.4.1. Photocatalysis

Despite the plethora of application already investigated in the field of SCNPs-based catalysis, still little effort has been put by the scientific community in the direction of photocatalysis. In the present work, we will try to exploit the potential of SCNPs architectures with photocatalysis, which represents a unique class of chemical transformations. Utilizing the energy delivered by light, opens new mechanistic routes for the reactants, driving reactions that are difficult, or sometimes even impossible, to carry out in the dark. When used for thermodynamically uphill reactions such as water splitting, photocatalysis promises as well a sustainable solution to large scale solar energy storage. Despite the longstanding interest in this process and research efforts, existing photocatalysis demonstrations are limited to academic laboratory settings. For the purpose of effective light absorption, charge separation, and charge transfer, a large number of photocatalytic materials, including conventional semiconductors and emerging photoelectronic materials such as nanoscale plasmonic metal particles, quantum dots, and 2D materials, have been studied.[18] Chief among the reasons for the slow progress, is the lack of suitable photocatalyst materials for large scale applications.

To this respect, we choose to focus on a particular class of photocatalytic process, the photoinduced RAFT polymerization. As recently reported, photo-RAFT polymerizations could constitute an effective, more oxygen-tolerant alternative to classical RAFT polymerizations.[19, 20] As the molecules which are used as photosensitizers are not soluble in aqueous environments, the major constraints associated with those reactions is the use of organic solvents.

The synthesis of novel, photocatalytically active SCNPs could provide a new platform to perform in more sustainable media those same reactions, which are commonly performed in organic solvents, as well as enhance the reusability and efficiency of the own catalysts.

2. Instrumental techniques

The main techniques used to characterize the prepared materials of this work are detailed below: Dynamic Light Scattering (DLS), Size Exclusion Chromatography (GPC/SEC) and Proton Nuclear Magnetic Resonance (^{1}H RMN).

2.1. Nuclear Magnetic Resonance (NMR)

The NMR is a non-destructive technique in which an external magnetic field, induces the excitation of the cores and where electromagnetic radiation above 10^{-3} nm (radio frequency) is employed to promote transitions between the lowest energy stage (α) and the highest energy state (β) (Figure 5).

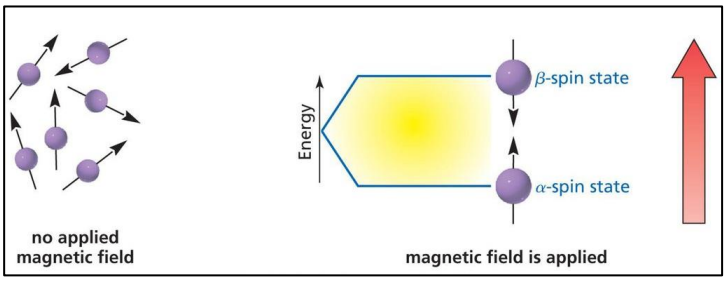

Figure 5: Spin-state division scheme when a magnetic field is applied.

The resonance frequency depends on the magnetic field surrounding the atom, and therefore gives us information about the chemical structure. If we use different magnetic fields we would expect different bands for the same molecule. This is why the frequency of a nucleus in relation to the reference is defined as chemical shift (δ) (Eq 1).[21]

$$\delta = \frac{\upsilon_{sample} - \upsilon_{ref}}{\upsilon_{ref}}$$

Eq 1: Chemical shift calculation.

With NMR technology many nuclei can be observed (e.g. ^{1}H, ^{13}C, ^{15}N or ^{19}F) being ^{1}H NMR and ^{13}C NMR are the most ones to analyse the structure and the chemical composition of polymeric materials. In this project, all ^{1}H NMR spectra were acquired in a Bruker 400 MHz at room temperature using deuterated chloroform ($CDCl_3$) as solvent.

2.2. Size Exclusion Chromatography (GPC/SEC)

The size exclusion chromatography is commonly used with polymers. An organic solvent such as tetrahydrofuran (THF), N,N-dimethylformamide (DMF) or chloroform ($CHCl_3$) can be used as the mobile phase. Compounds are separated using size as a filter, considering that the compounds will split between the mobile phase and the stationary phase.

The GPC/SEC it is a very good technique for the determination of values such as M_w, M_n and $Đ$ (Eq 2-4).

$$M_w = \frac{\sum_i N_i \times M_i^2}{\sum_i N_i \times M_i}$$

Eq 2: Weight average molecular weight determination.

$$M_n = \frac{\sum_i N_i \times M_i}{\sum_i N_i}$$

Eq 3: Weight average molecular weight determination.

Where N_i is the number of *i* molecules and M_i is the molecular weight of those molecules.

$$Đ = \frac{M_w}{M_n}$$

Eq 4: The formula for the calculation of dispersity.

In general, a GPC instrument is formed by: a pump, a chromatographic column (stationary phase), a solution (mobile phase), detectors and a computer processing unit. The stationary phase is a porous matrix that separates the compounds depending on the size of the particles. The interior of the column is made up of pores of different sizes. If the particle is the right size it will pass through these pores increasing the elution time. On the other hand, if the particle is too large to pass through these pores, it will leave the column earlier.[22]

In this work, GPC/SEC measurements were carried out at 30°C using THF as solvent, on an Agilent 1200 (Figure 6) equipped with a MALLS (MiniDraw Treos, Wyatt) detector, a differential refractive index (RI) (Optilab Rex, Wyatt) detector and a viscosimeter detector (ViscoStar-II,Wyatt). For the interpretation of the obtained results, we used 6.1 version of ASTRA Software.

Figure 6: Picture of the 1200 Agilent chromatograph and different detectors used in this project.

A GPC running in DMF as solvent was also used. The chromatograph contains a triple-detection Agilent PL-GPC 50 system (Figure 7) with Agilent light scattering, refractive index and viscosimetry detectors- equipped with PL aquagel-OH Guard (8µm) and PL aquagel-OH MIXED-H (8µm) columns. Data analysis was performed with the Agilent GPC/SEC software.

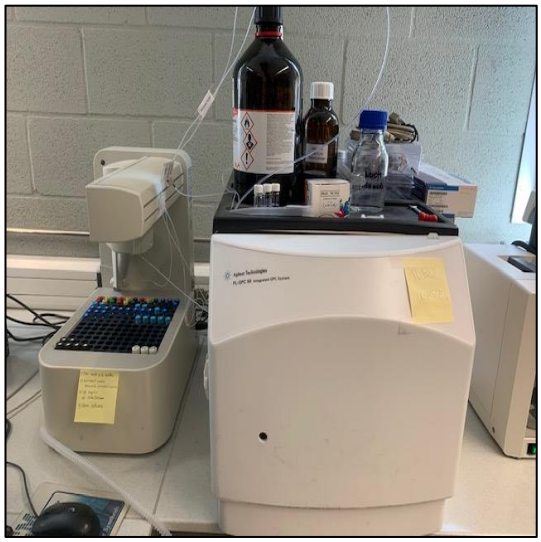

Figure 7: Picture of the Agilent-GPC 50 used in this work.

2.3. Dynamic Light Scattering (DLS)

Dynamic Light Scattering (DLS) is a non-destructive technique that bring us information about the nanometric molecules (polymers, micelles…) behaviour and size distribution in a solution. The DLS is incorporated with a laser which illuminate the solution which lead to a dispersed signal; this dispersed light is detected by the detectors. These detectors are located at a known angle.

Due to the Brownian movement the scattered light suffers fluctuations, these fluctuations can be determined by the use of a correlation function. To study the speed in which the intensity fluctuates a digital correlation is applied.

The diffusion of the particles (D) and the hydrodynamic radius (R_H) are related in the Stokes-Einstein equation (Eq 5). R_H is the parameter that shows the radius a sphere with the same diffusion coefficient would have in solution.

$$D = \frac{K_B T}{6\pi\eta R_H}$$

Eq 5: Stokes-Einstein equation: Where, KB is the Boltzmann constant, η is the viscosity and T is the temperature of the measures.

A DLS equipment is composed by a laser, detectors, attenuator, cell and the processing software. The laser is the light source. The detectors are positioned in such a way that they only detect 90° and 173° dispersions, measuring the scattered signal. The attenuator controls the intensity of the laser Finally, the cell is used to deposit the sample and the correlator transfers the information to the computer.

Particularly in this project, a Malvern Zetasizer Nano Zs instrument (Figure 8) was used to determine the R_H of the performed materials. The DLS measurements were carried out at 25°C using different solvents such as water (H_2O) and tetrahydrofuran (THF) to determine the R_H. The refractive index and the viscosity of the used solvents are important parameters to evaluate correctly the R_H and they are already described in literature.[23]

Figure 8: Picture of the DLS instrument used in this project: Malvern Zetasizer DLS.

3. Objectives

The main goal of this work is to achieve a more controlled, photo-induced, RAFT polymerization in aqueous media. For this purpose, this project was focused on the design and synthesis of a new, water-soluble and photo-active nanoreactor to be used as a potential photocatalyst in aqueous RAFT polymerizations.

First, we selected a cyclometalated Ir (III) complex as photosensitiser (PS) which already demonstrated to have excellent catalytic activity in the photo-polymerization of NIPAM using organic solvents.[19]

In order to perform this reaction in water, we designed and prepared a polymeric precursor, which simultaneously could be water-soluble and suitable for the coupling with the PS. We focused on the preparation of an amphiphilic copolymer, Poly[(OEGMA)-*r*-(AEMA)] (POA1) *via* RAFT copolymerization. Then, we optimized the PS anchoring reaction, exploiting the chemical characteristics of the hydrophobic, β-ketoester groups in the lateral chain of the precursor.

Once obtained the photo-active polymer, its hydrodynamic behaviour in aqueous and organic media was determined by dynamic light scattering techniques, in order to assess its stability and conformational states in the different environments investigated.

The obtained water-soluble Ir (III)-containing SCNPs were finally used to perform aqueous photo induced RAFT polymerization of N-isopropyl acrylamide (NIPAM), its catalytic activity and efficiency were evaluated and compared with the non-supported Iridium complex PS.

4. Experimental

4.1. Materials and methods

Chemicals and reagents:

Oligo(ethiyleneglicol) methyl ether methacrylate (OEGMA, 95%), 2-acetoacetoxy ethyl methacrylate (AEMA, 95%) were received from Aldrich and were purified with basic alumina. 4-cyano-(phenylcarbornothioylthio)pentanoic acid (CPADB, >97%), 2,2-azobis(2-methylpropinitrile) (AIBN, >98%) were received from Aldrich and were purified by recrystallization. Dichloromethane (DCM, synthesis grade), chloroform ($CHCl_3$, synthesis grade), tetrahydrofuran (THF, analytical grade), hexane and methanol (analytical grade) were received from Scharlab. 1,4 Dioxane (99.8%), ethyl acetate (synthesis grade), N-isopropylacrylamide (NIPAM, >99), deuterated chloroform ($CDCl_3$, 99.8%) and potassium hydroxide (KOH, reagent grade) were supplied by Sigma-Aldrich. As for the deionised water used in this work, it has been obtained from the apparatus Thermo Scientific (Barnstead TII Pure Water System). $[Ir(ppy)_2OH]_2$ and $[Ir\ (ppy)_2(meacac)]$ were synthetized by the Freixa´s Group (UPV/EHU).

Equipments:

^1H NMR spectra were recorded on a Bruker 400 MHz spectrometer in appropriate deuterated solvents (in this work, all measurements were performed in $CDCl_3$). Chemical shifts are given in ppm (δ) relative to the $CDCl_3$ (7.26 ppm for ^1H NMR) Dynamic light scattering (DLS) experiments were performed (at two different angles 90° and 173°, with a sample concentration of 1 mg/mL in water and THF) using a Malvern Zetasizer Nano. Molecular weights and dispersity were determined by gel permeation chromatography (GPC) using a Agilent serie 1200 chromatographer equipped with PLgel Mixed LS precolumn and with 3 detectors 1) for viscosity; ViscoStar-II Wyatt, 2) for the MALLS; MiniDawn Treos, Wyatt, 3) for the refractive index; Optilab Rex, Wyatt), THF was used as the mobile phase at a flow rate of 1 mL/min.

SEC measurements of Poly(N-isopropylacrylamide) were performed at 30°C on a triple-detection Agilent PL-GPC 50 system with Agilent light scattering, refractive index and viscosimetry detectors- equipped with PL aquagel-OH Guard (8µm) and PL aquagel-OH MIXED-H (8µm) columns, using N,N-dimethylformamide (DMF) as mobile phase

For the photopolymerization we used 2 equipments (Figure 9): 1) a Photoreactor m2 from Penn PhD and 2) a Spot Light Source LC8 from Hamamatsu.

1) Photoreactor m2 was used at maximum intensity (3.4 W/cm^2) to accelerate and photocatalyzed reactions at 420 nm. This equipment it is equipped with a parameter controller for the control of temperature, stirring and light intensity. The temperature feedback is due to a K-type thermocouple. The Photoreactor m2 it is equipped with a sensor that stops the light irradiation when the light shield is opened.

2) Spot Light Source LC8 was used at maximum intensity (4.5 W/cm^2) with super-quiet mercury-xenon lamp (L10852) in order to photocatalyzed reactions between 200 and 400 nm.

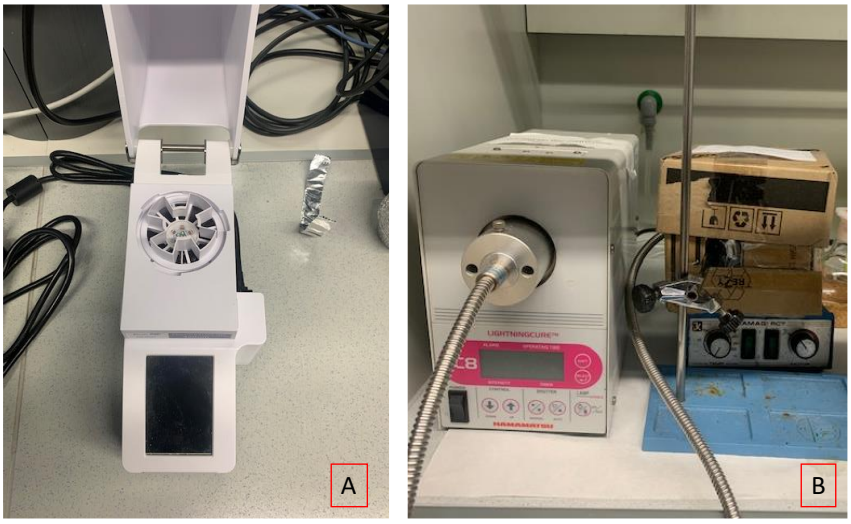

Figure 9: A) Photoreactor m2. B) Spot Light Source LC8.

4.2. Synthesis

Synthesis of the copolymer Poly[(OEGMA)-r-(AEMA)], POA1

OEGMA (1.575 g, 1.5 ml, 5.25 mmol), AEMA (0.375 g, 0.34 ml, 1.75 mmol), CPDB (9.5 mg, 3.4x10^{-2} mmol) and AIBN (1.1 mg, 7x10^{-3} mmol) were dissolved in 1,4-dioxane (2.9 mL). The reaction mixture was degassed by flushing Argon for 15 minutes. The copolymerization reaction was carried out at 70°C for 24 h. After this time, the crude of reaction was cooled down in a liquid nitrogen bath for twenty minutes. Then, the mixture was heating up to room temperature (r.t) and 2mL was added in the mixture. The purification of the copolymer was performed by several precipitations in a large excess n-hexane, until a complete removal of the residual monomers was reached. At this point, the isolated product was dried under vacuum in an oven at r.t. for 24 hours. The product was obtained as a slightly pink viscous material (**POA1**, 1.814 g, yield: 93 %). This material was characterized by ^{1}H NMR and GPC/SEC. POA1: ^{1}H NMR (400 MHz, $CDCl_3$): δ 4.35 (4H, O-CH_2-CH_2-O-CO-); 4.09 (8H, O-CH_2-CH_2-O-CO and O-CH_2-CH_2-O); 3.66 (2H,OC-CH_2-CO-); 3.38 (3H, CH_3-O-); 2.31 (3H, CH_3-CO-); 1,79 (4H, 2x -CH_2-C-CH_3); 1.02-0.87 (6H, 2x -CH_2-C-CH_3). GPC/SEC: M_w=103.8 kDa/mol, $Đ$ = 1.04.

Synthesis of P[(OEGMA)-r-([Ir]/AEMA)], POA1-Ir

POA1 (50 mg,4.4x10^{-4} mmol) and [Ir(ppy)$_2$OH]$_2$ (5.3 mg, 5x10^{-3} mmol) were weighted in a 10 mL glass vial. Then, 6 mL of DCM were added into the vial. The vial was sealed with a rubber septum and, using a needle, the solution was bubbled with Argon for 10 minutes. The mixture of reaction was stirred at room temperature for 4 days. The reaction was real-time monitored by ^{1}H NMR spectroscopy. The performed reaction resulted to be quantitative after 4 days and no further purification of the product (**POA-Ir**) was necessary. **POA1-Ir** was obtained as a deep yellow solution (55.3 mg, yield: 100%). This material was characterized by ^{1}H NMR and GPC/SEC. ^{1}H NMR (400 MHz, $CDCl_3$): δ 8-6.22 ppm (8 H, aromatic protons) 4.33 (4H, O-CH_2-CH_2-O-CO-); 4.07 (8H, O-CH_2-CH_2-O-CO and O-CH_2-CH_2-O); 3.64 (2H,OC-CH_2-CO-); 3.37 (3H, CH_3-O-); 2.3 (3H, CH_3-CO-); 1,82 (4H, 2x -CH_2-C-CH_3); 1.02-0.87 (6H , 2x -CH_2-C-CH_3). GPC/SEC: M_w =120 kDa/mol, $Đ$ = 1.05.

General procedure for the synthesis of PNIPAM

377 µL of a stock solution of POA1 or [Ir(ppy)$_2$(meacac)] in THF (5.3 mg/mL) were added into a 10 mL oven-dried vial. After solvent removal via argon fluxing, 9.3 mg (3.3x10^{-2} mmol) of 4-cyano-4-(phenylcarbonothioylthio)pentanoic acid (CPADB), 487 mg (4.3 mmol) of N-isopropyl acrylamide (NIPAM) and 2 mL of water were added. The resulting mixture was degassed flushing Ar for 10 minutes and sealed with a rubber gum septum. The reaction mixture was then stirred at r. t. and exposed to LED light (200-400 nm) for 19 hours. The crude was then analyzed by GPC/SEC (DMF, LiBr 0.1 %) and ^{1}H NMR. The polymer was precipitated in cold methanol and dried under vacuum at r.t. PNIPAM was obtained as a deep yellow viscous material. This material was characterized by GPC/SEC (DMF, LiBr 0.1 %) and ^{1}H NMR. ^{1}H NMR (400 MHz, $CDCL_3$):δ 4 ppm (1H, -NH-CH-(CH_3)$_2$); 1.85 (1H, -CH_2-CH-CO-); 1.27 (2H, -CH_2-CH-CO); 0.89 and 0.88 (6H, 2x CH_3-CH-NH-). GPC/SEC: M_w =37.34 kDa/mol, $Đ$ =1.568.

5. Results and discussion

5.1. Synthesis and characterization of POA1

Following a similar synthetic procedure described by the Pomposo's group,[23] an amphiphilic random copolymer of oligo(ethylene glycol) methyl ether methacrylate (OEGMA, hydrophilic) and 2-acetoacetoxy ethyl methacrylate (AEMA, hydrophobic) (P(OEGMA-*r*-AEMA), POA1) was prepared (Figure 10). It was synthesized via RAFT copolymerization using AEMA and OEGMA as monomers, 4-cyanopentanoic acid dithiobenzoate (CPADB) as chain transfer agent (CTA) and 2,2-azobis(2-methylpropionitrile) (AIBN) as radical initiator. POA1 was obtained with a 93% yield, presenting 17% of AEMA units and a weight average molecular weight (M_w) of 103.8 kDa and a dispersity index ($Đ$) of 1.04 (Table 1).

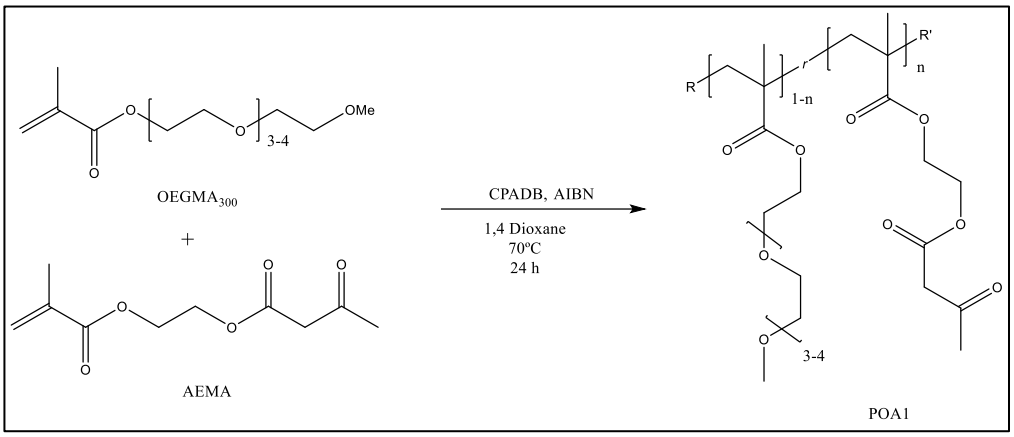

Figure 10: Synthetic scheme for the preparation of POA1. Reaction conditions: [M]/[CPADB]/[AIBN] =200:1:0.12, 1,4-dioxane, 70 °C, 19h, inert atmosphere.

The M_w, M_n and $Đ$ of POA1 were determined by GPC-dRI-VS-LS analysis (Figure 11). The $Đ$ value measured reflects a good homogeneity of the sizes of the polymer chains, in agreement with a classical controlled radical polymerization (Table 1).[24] As we were interested in the preparation of non-covalent, globular SCNPs, this copolymer resulted to present a suitable value of M_w for the preparation and evaluation of the formation of SCNPs. As a matter of fact, it can be experimentally observed that the longer the polymer chain, the easier is to detect its collapse into a globular, or a sparse, single chain nanoparticle.

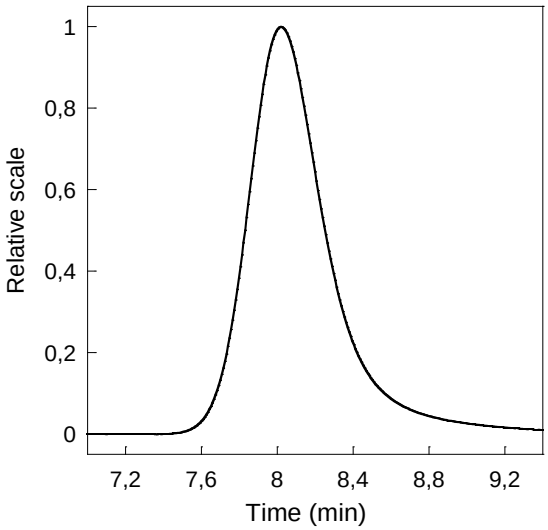

Figure 11: SEC data of POA1 (dRI chromatrogram in THF).

Table 1: Values of M_n, M_w and $Đ$ for POA1.

Entry	*[M]:[CPADB]:[AIBN]*	*M_n (kDa)*	*M_w (kDa)*	*$Đ$*
POA1	103:1:0.2	99.5	103.8	1.04

The chemical structure and composition in terms of monomer ratios of POA1 was confirmed by quantitative ^{1}H NMR, $CDCl_3$ as solvent (Figure 12).

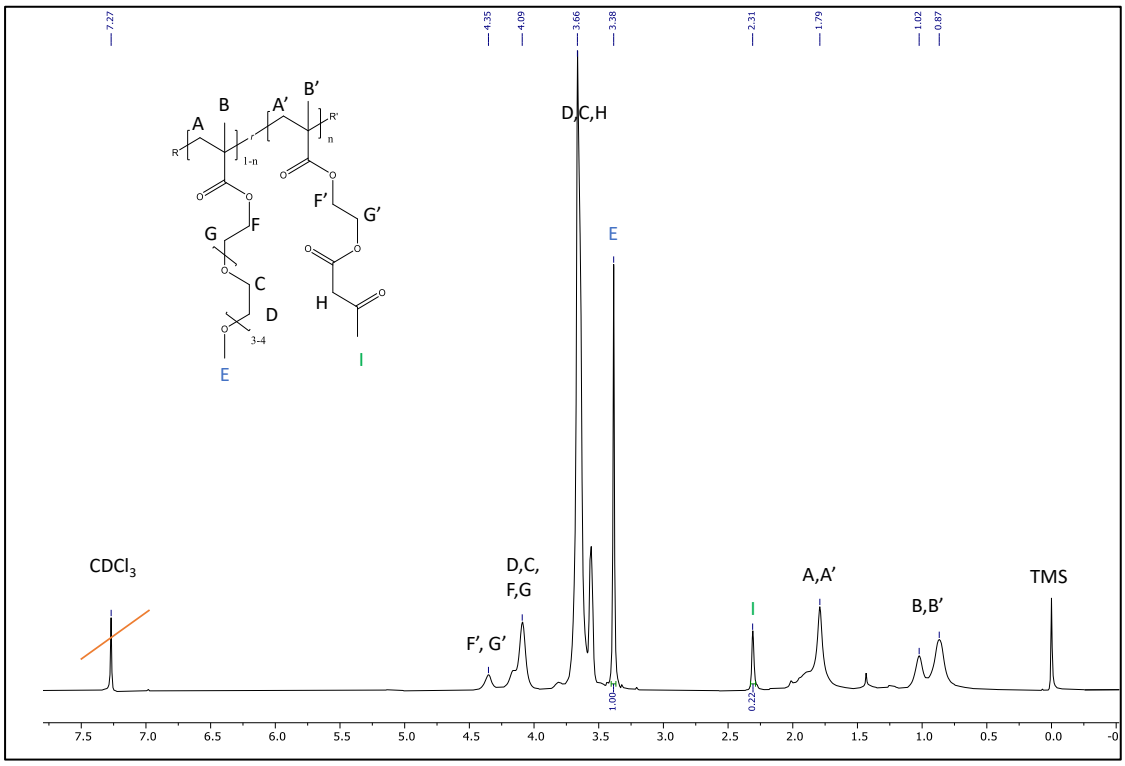

Figure 12: ^{1}H NMR spectrum of POA1 in $CDCl_3$.

The peak I at 2.31 ppm corresponds to the protons of the methyl group in the alpha position to the ketone (CH_3-C=O) of the AEMA moiety in the lateral chain of the polymer. Moreover, the peak labeled as E and located at 3.38 ppm, is assignable to the protons of the methoxy functional group (CH_3-O) of OEGMA. The percentage of each monomer in the copolymer was determined using the ratio between the area of the peak I (AEMA) and peak E (OEGMA) as specified in Equation 6. The copolymer POA1 presented 17% of AEMA and 73% of OEGMA.

$$\%AEMA_{mol\%} = \frac{S^I}{S^I + S^E} 10^2$$

Eq. 6: Equation used to determine molar percentage of AEMA functional group in the copolymer, in which S^n corresponds to the normalized signal intensity of the n-signal in the ^{1}H NMR spectrum (n = I for AEMA, n = E for OEGMA).

The hydrodynamic radius (R_H) was measured by dynamic light scattering (DLS). In this case, the size distributions by number of the aggregates populations of the copolymer POA1 were determined in two different solvents (water and tetrahydrofuran) and at the same polymer concentration (1 mg/mL). In THF, a non-polar solvent, the polymer chains are randomly dispersed. As THF is a very good solvent for both the comonomers, the polymer is perfectly solubilized and organized in linear, random-walk-like, conformation (R_H = 3.8 nm). In water, the copolymer tends to hide the hydrophobic moieties present in the lateral chain (AEMA groups), and spontaneously self-organizes itself in a globular, core-shell, SCNPs (R_H = 3.3 nm). As reported in Figure 13, switching from the THF (linear, more extended conformational state) to water (globule-like, more compact state, SCNP) the SCNPs formation can be confirmed by the reduction in the hydrodynamic radius, which corresponds to the collapse of a single polymer chain, induced by the sole solvophobic interaction of the hydrophobic residues in the POA1.

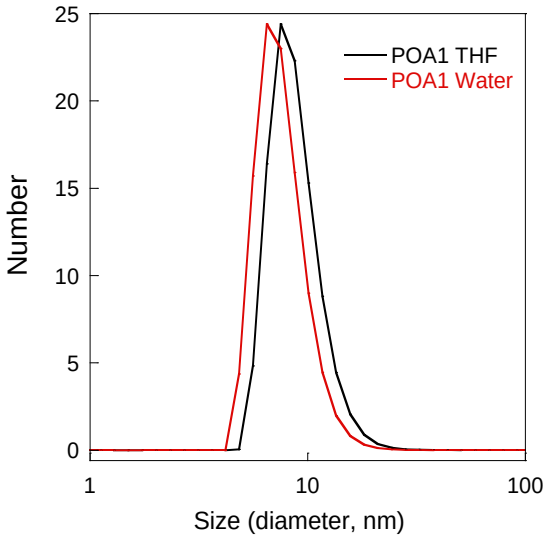

Figure 13: Measurements (by Number) obtained by DLS of POA1 solutions, at a polymer concentration of 1 mg/mL, both in THF (black line) and water (red line). All the measurements were obtained as an average of at least four consecutive acquisitions.

5.2. Synthesis and characterization of POA1-Ir

Once isolated and characterized the polymeric scaffold (POA1), we tried to transform it into a photo-active copolymer, via a post-polymerization functionalization approach. In order to do so, we choose to take advantage of the chemistry of β-ketoesters, anchoring an Iridium (III) cyclometallated complex to the AEMA moieties. As shown in the synthetic scheme in Figure 14, the Iridium (III) functionalization of POA1 was achieved via a simple ligand exchange reaction with the bimetallic dimer $[Ir(ppy)_2OH]_2$. As a matter of fact, the reaction of the AEMA group with the hydroxo-bridged dimer $[Ir(ppy)_2OH]_2$ is spontaneous, as is both entropically (chelation effect) and enthalpically favoured (formation of two molecules of water). For these reasons, the use of the hydroxo-bridged dimer allowed us to carry out the reaction in very mild conditions (DCM, room temperature).

The reaction was performed dissolving the polymer precursor POA1 and $[Ir(ppy)_2OH]_2$ (1 equivalent) in dry dichloromethane. The resulting solution was then left stirring under inert atmosphere and at room temperature for four days. After this time, the product POA1-Ir was isolated and recuperated in a quantitative way via complete elimination of the solvent. POA1-Ir was then characterized via GPC/SEC and quantitative ^1H NMR (Figures 14 and 15).

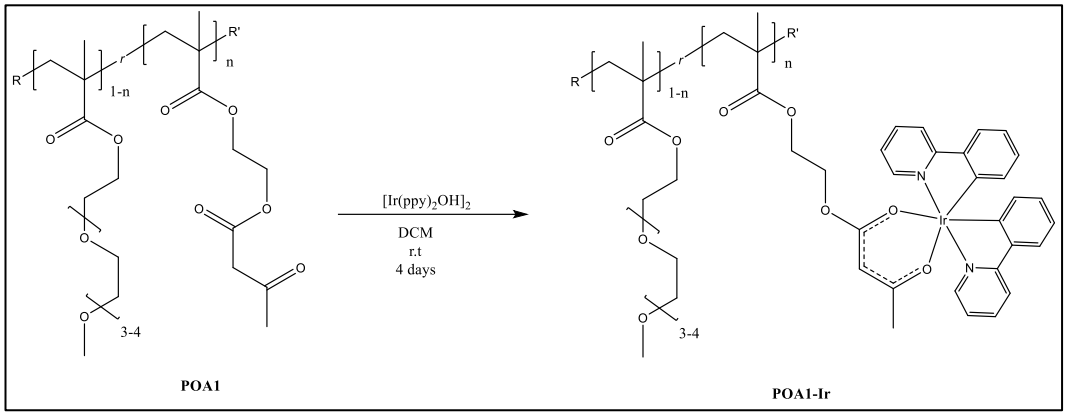

Figure 14: Synthetic scheme for the preparation of POA1-Ir. Reaction conditions: DCM, r.t., stirring for 4 days.

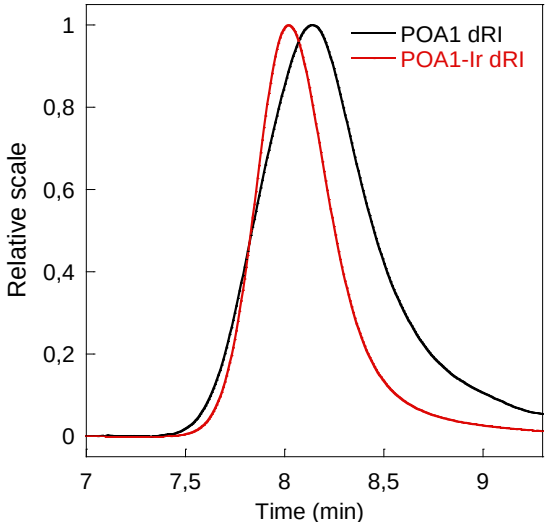

Figure 15: Comparison of the dRI results obtained for POA1 and POA1-Ir by GPC in THF.

From the GPC/SEC analysis of POA1-Ir and from the comparison with its precursor POA1, we observed an increment in the number average molecular weight distribution. As shown in Figure 15, after the anchoring reaction of the Iridium complex, as expected the M_w increases. Nevertheless, we could not employ the ΔM_w as a reference value for the quantification of the Iridium in the polymer because of the uncertainty on the different elution behaviour of the two polymers in the chromatographic system.

Supported by literature data, we assumed a quantitative modification of the AEMA group.[25] As it emerges from NMR analysis (Figure 16), in the aromatic region of the spectrum (6-9 ppm) some characteristic signals of the ligands of the Iridium complex appear after the functionalization reaction, confirming the effectiveness of the anchoring protocol.

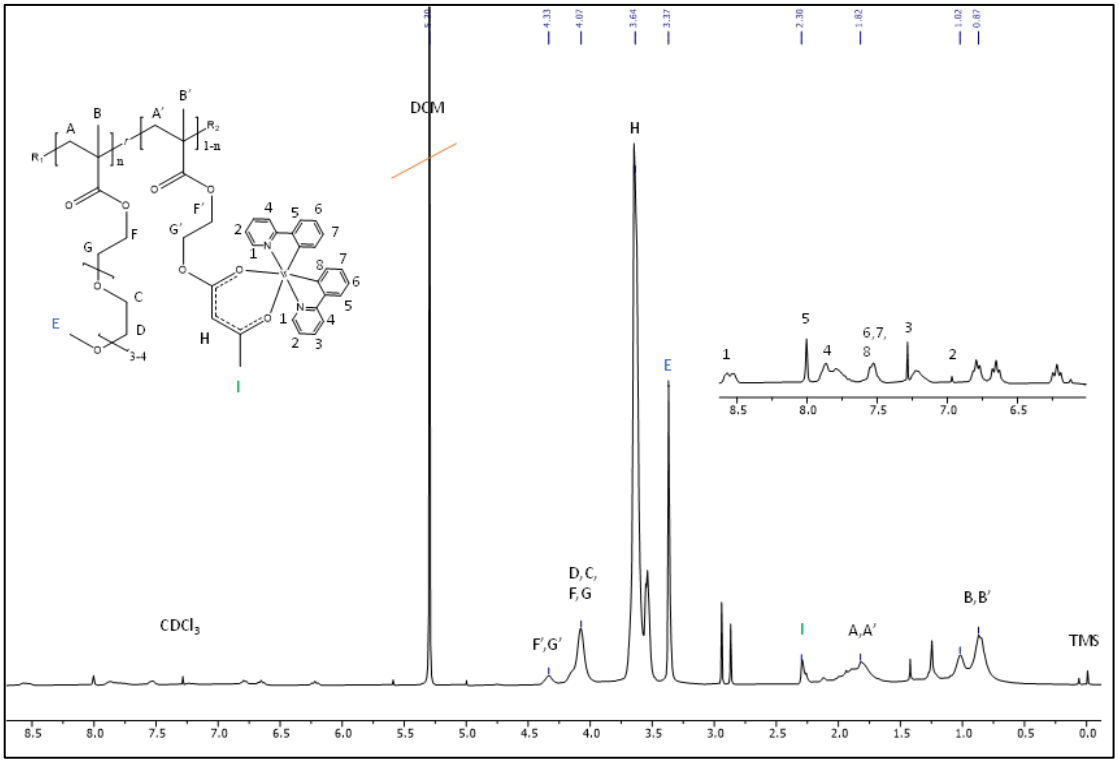

Figure 16: ^{1}H NMR spectrum of POA1-Ir in $CDCl_3$.

In the Figure 16, all the characteristic signals of the polymer precursor POA1 are present, indicating that no significant chemical modification occurred at the level of the main chain, nor in the lateral OEGMA groups.

The quantification of the Iridium content in the polymer could not be evaluated by NMR spectroscopy. The aromatic protons are not relaxing properly to enable the quantification and no other clear signals that can be assigned to the complex are resolved in the spectrum. We could only confirmed that the signals present in the aromatic region (8.7-6 ppm) are the same as found for the model compound $Ir(ppy)_2(acac)$. Inductively Coupled Plasma-Mass Spectroscopy (ICP-MS) analysis will be carried out in order to determine the Iridium content (ongoing) of POA1-Ir. For this reason, we assumed that the quantitative (mol) of Iridium complex in the polymer is the same as the initial amount of AEMA in the precursor.

For the characterization of the hydrodynamic behaviour of POA1-Ir, we measured the values of R_H (nm) from polymer solutions via DLS. As well as for the precursor, for the functionalized polymer switching from the THF to water a reduction in the hydrodynamic radius was observed, which corresponds to the collapse of a single polymer chain (Figure 17).

Interestingly, the collapse observed in the POA1 is 0.5 nm, and in the case of the Iridium-containing polymer underwent to a reduction in R_H of about 0.4 nm (Figure 17), indicating that

the anchoring of the Iridium to the hydrophobic lateral groups did not affect significantly the self-assembly properties of the material.

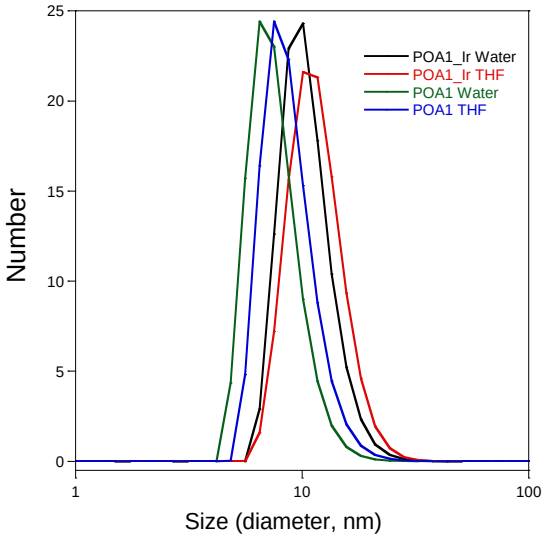

Figure 17: Comparison of DLS measurements of POA1 and POA1-Ir solutions both in water and in THF, all at a polymer concentration of 1 mg/mL.

After the synthesis and characterization of these new photoactive nanoreactors, their photo catalytic activity was explored for the polymerization of NIPAM in water.

5.3. Photopolymerization of NIPAM

We wanted to exploit the catalytic potential of the POA1-Ir-based SCNPs, merging the photosensitization conferred by the Iridium (III) in the lateral chain and the amphiphilicity of the polymeric scaffold.

In order to do so, we choose the RAFT photopolymerization of the commercially available monomer N-isopropyl acrylamide (NIPAM). We performed a series of photo-induced polymerization in water, using CPADB as chain transfer agent. Contrarily to classic, thermal RAFT polymerizations, in the case of photo-activated RAFT there is no need of any thermal free-radical initiator. The main results are summarized in Table 2.

Table 2: Data of the prepared PNIPAM. The code of each polymer, the used photocatalyst and the light wavelength, proportions, M_W and $Đ$ is showed in the table.

Entry	*Photocatalyst*	*[NIPAM]:[CPADB]:[Ir]$_\vartheta$*	*λ_{max} (nm)*	*M_w (kDa)*	*$Đ$*
PNIPAM1	POA1-Ir	200:1:0.12	200-400	87	1.87
PNIPAM2	No photoactive specie	200:1:-	200-400	97	2.05
PNIPAM3	No photoactive specie	200:1:-	420	338	5.63
PNIPAM4	POA1-Ir	200:1:0.12	420	37	1.56
PNIPAM5	[Ir(ppy)$_2$(meacac)]	200:1:0.12	420	57	2.39

The RAFT polymerization reactions of NIPAM were monitored by GPC and ^{1}H NMR experiments were carried out to confirm the formation of PNIPAM. A strength of photoredox catalysis lies in the ability to generate reactive open shell intermediates via single electron transfer (SET) in a controlled manner and under mild conditions. The photosensitizer is converted into a reactive species, which can act as a strong oxidant or as strong reductant, after been excited. This circumstance permits to selectively add energy to a light-harvesting system, as most organic substrates/ reagents do not absorb in the visible region of the electromagnetic spectrum. This fact is in contrast to irradiation with ultraviolet (UV) light where deleterious radical side reactions can occur through substrate/ reagent photoexcitation, and heating where energy is applied uniformly to the system.[26] For these reasons, the catalyst for a photoredox system is chosen based on a variety of factors, including (but not limited to) substrate redox potential(s), catalyst redox properties, excited state lifetime, or possible catalyst degradation pathways. As the knowledge of catalyst, cocatalyst, substrate, and reagent redox potentials allows one to predict the thermodynamic feasibility of electron transfer (and by means, of the reaction itself), we measured the absorption spectra of the POA1-Ir in water via UV-Vis spectrophotometry (Figure 18).

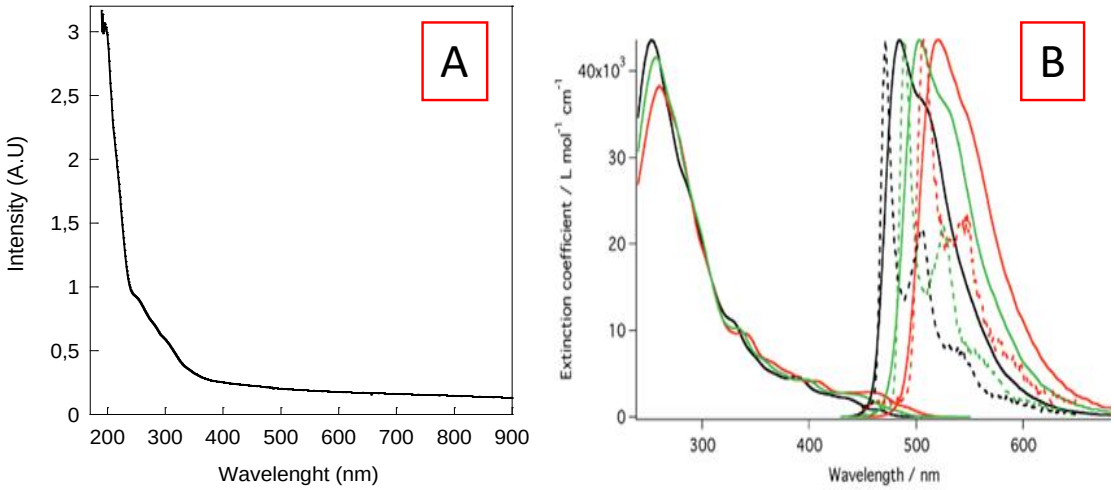

Figure 18: Comparison between the UV-Vis absorption spectra of POA1-Ir (*A*), prepared for this work, in water ([polymer] = 1 mg/mL) and $Ir(ppy)_2(meacac)$ in DCM; (*B*), from literature data.[27]

As it can be appreciated from the UV absorption spectra, the polymer-supported Iridium (III) photocatalyst presents a similar behaviour when dissolved in water if compared with the model compound $Ir(ppy)_2(meacac)$ in DCM, which constitutes a first indication that our system could be used to perform the reaction we were interested in. While POA1-Ir can self-organize itself in aqueous media in a SCNP conformation, $Ir(ppy)_2(meacac)$ is indeed completely insoluble in water when not supported on the polymer and all the data present in literature are measured from organic solvent solutions. Light absorption of the photosensitizer served us as a crucial information with respect of reaction feasibility, and allowed us to choose the correct wavelength range of irradiation. Because of these reasons, we firstly tried to perform the RAFT photopolymerization of NIPAM using an intense light source (4.5 W/cm^2) with a broad range of emission (200-400 nm). Following this procedure, two different polymers were obtained depending on the photocatalyst used in the reaction, PNIPAM1 and PNIPAM2 (respectively, in presence and in absence of the photosensitizer). The Figure 19 shows the dRI chromatograms of PNIPAM1 and PNIPAM2 in DMF. Both chromatograms are similar; consequently, they present similar M_w and $Đ$. The similar peaks indicate that the reaction is due to an unexpected process, which is not dependent on the presence nor absence of the photosensitizer. After to observe these results, we hypothesized a photo-induced spontaneous cleavage of the CTA, which is capable of acting simultaneously as initiator and chain transfer agent (IniFerTer process)[28] under the UV conditions we were using. In order to avoid this effect, we decided to switch to longer wavelength and to lower the light source intensity using a blue LED light (λ_{max} = 420 nm).

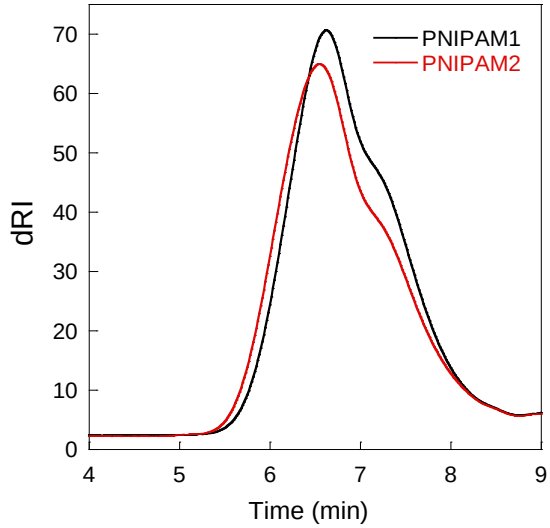

Figure 19: dRI chromatograms of PNIPAM1 (black line) and PNIPAM2 (red line) synthetized in water with a 200-400 nm light.

When the polymerization is performed in aqueous media and with blue LED as light source (3.4 W/cm^2, λ_{max} = 420 nm), we observed a peculiar difference between the final products, depending on the photocatalyst used. As it can be observed in Figure 20, when employing the free Iridium (III) complex [Ir(ppy)$_2$(meacac)], a high molecular weight, very disperse product was obtained (PNIPAM5). Nevertheless, using the prepared photocatalytic single chain nanoparticle (POA1-Ir) as the photosensitizing agent, a lower M_w and $Đ$ of the final PNIPAM (PNIPAM4) was obtained. In order to confirm that no secondary reactions were interfering with the final products of these last experiments, we performed an additional control reaction in total absence of any photocatalyst. As expected, in this case, almost no product formation was observed, as the majority of the isolated product resulted to be residual monomer and some impurities (Figure 21). Only a small amount of a very disperse ($Đ$ = 5.63) polymer was obtained (PNIPAM3), confirming that these polymerization conditions were suitable for this purpose.

From the comparison of the molecular weight distributions of PNIPAM4 and PNIPAM5, we hypothesized that the single chain nanoparticle photocatalyst was able to enhance the efficiency of a RAFT photopolymerization in water. Opposite to the free Ir-complex, which is insoluble in water, the amphiphilic copolymer (POA1) is able to stabilize the photoactive species in the hydrophobic core of their structure, acting as a core-shell nanoreactor.

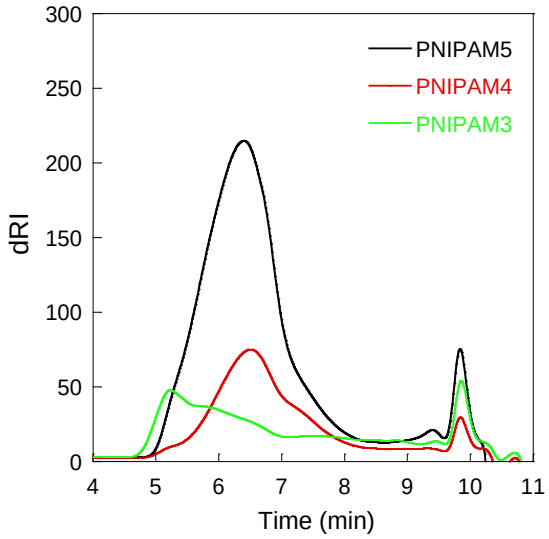

Figure 20: dRI chromatogram of PNIPAMs synthetized in water at λ_{max} = 420 nm**.**

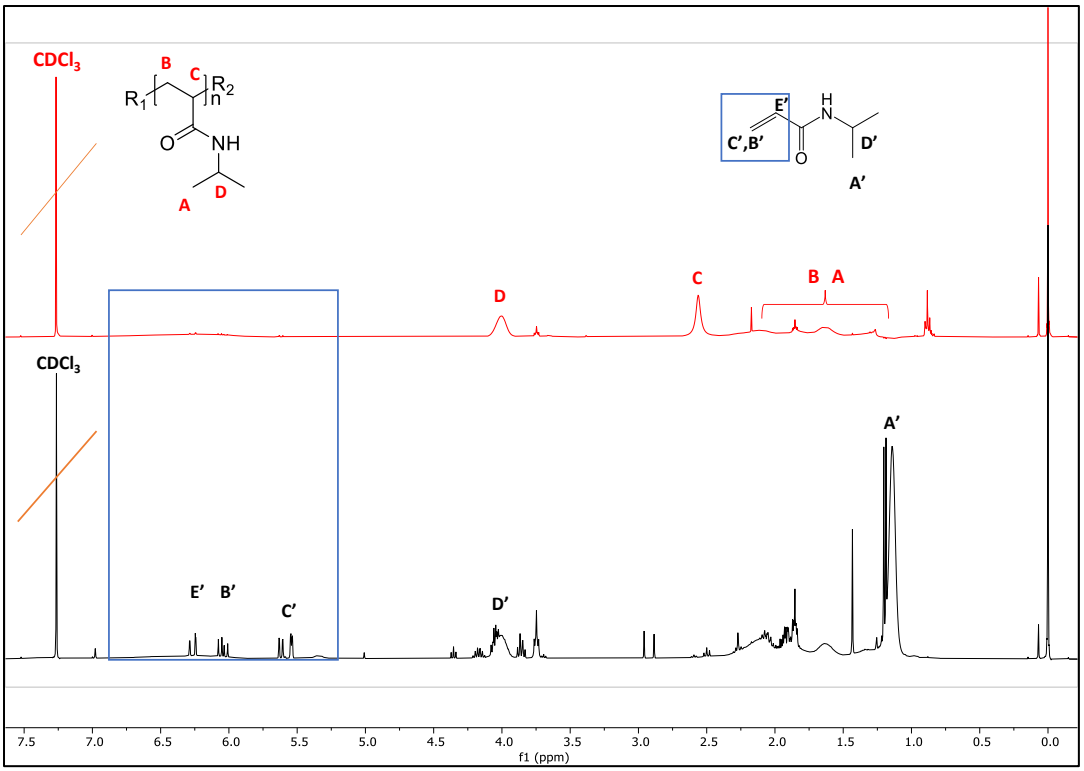

Figure 21: ^{1}H NMR spectra of PNIPAM3 and PNIPAM4 in $CDCl_3$. The red line corresponds to the spectrum of PNIPAM4 and the black line corresponds to the spectrum of PNIPAM3.

The polymers were purified via three consecutive precipitations in n-hexane and then dried under dynamic vacuum until complete solvent removal. The structure of the prepared PNIPAMs were confirmed by ^{1}H NMR in deuterated chloroform. For clarity, we report only a comparison between PNIPAM4 and PNIPAM3, as all the spectra resulted to be similar.

In the case of the material obtained in the reaction without photocatalysts (PNIPAM3), a very low yield (mass) was obtained and the isolated product resulted to be a hardly soluble solid. The Figure 21 shows the comparison of the two obtained ^{1}H NMR spectra of the purified products, PNIPAM3 (no catalyst) and PNIPAM4 (POA1-Ir as catalyst), respectively. If we compare them, we can observe that in the case of PNIPAM3, without catalyst, monomer (signals between 5 and 7 ppm, vinylic region) and unknown impurities were obtained, indicating that the isolated material is not only PNIPAM, even after the purification. On the contrary, PNIPAM4 presented the typical ^{1}H NMR spectrum of PNIPAM, which in conjunction with the GPC/SEC data confirms us the controlled character of the reaction performed in presence of the photocatalyst.

6. Conclusions

In this work, we obtained preliminary results in achieving a more controlled, photo-induced, RAFT polymerization in aqueous media. For this purpose, we synthesized a new, water-soluble and photo-active material (POA1-Ir) to be used as a potential photocatalyst in aqueous RAFT polymerizations.

We selected a cyclometalated Ir (III) complex as photosensitiser (PS) which already demonstrated to have excellent catalytic activity in the photo-polymerization of NIPAM using organic solvents.

In order to perform this reaction in water, we designed and prepared an amphiphilic copolymer precursor, Poly[(OEGMA)-*r*-(AEMA)] (POA1) *via* RAFT copolymerization. Then, we optimized the PS anchoring reaction, exploiting the chemical characteristics of the hydrophobic, β-ketoester groups in the lateral chain of the performed precursor, which yielded a P[(OEGMA)-*r*-([Ir]/AEMA)], nanoreactor (POA1-Ir).

Once obtained the photo-active polymer, its hydrodynamic behaviour in aqueous and organic media was determined by DLS, in order to assess its stability and conformational states in the different environments investigated.

The obtained water-soluble Ir (III)-containing SCNPs (SCNPs-Ir) were finally used to perform aqueous RAFT photopolymerization of N-isopropyl acrylamide (NIPAM), its catalytic activity and efficiency were evaluated and compared with the non-supported Iridium complex PS. Photo-induced RAFT polymerization of NIPAM in water from these novel single-chain nanoreactors results in the synthesis of Poly(NIPAM) of M_W =37.34 kDa, $Đ$ =1.56.

7. References

(1) Ileana Covaliu, C.; Jitaru, I.; Paraschiv, G.; Vasile, E.; Biris, S-S.; Diamandescu, L.; Ionita, V.; Iovu, H. *Powder Technology* **2013**, 237, 415.

(2) Liu, Y.; Turunen, P.; F.M. de Waal, B.; Blank, K.G.; Rowan, A.E.; Palmans, A.R.A.; Meijer, E.W. *Molecular Systems Design & Engineering* **2018**, 3, 609.

(3) Latorre-Sanchez, A.; Pomposo, J.A. *Chemical Communications* **2015**, 51, 15736.

(4) Gonzalez-Burgos, M., Latorre-Sanchez, A., Pomposo, J.A. *Chemical Society Review* **2015**, 4, 6122.

(5) Bonet, A.; Blaszczak, W.; Rosell, C.M. *Cereal Chemistry* **2006**, 83, 655.

(6) Tezuka, Y.; Oike, H. *Journal. American. Chemical. Society* **2001**, 47, 11570.

(7) Graeme, M.; Ezio, R.; Thang San H. *Australian Journal of Chemistry* **2005**, 58, 379.

(8) Sanchez-Sanchez, A.; Pérez-Baena, I.; Pomposo, J.A. *Molecule* **2013**, 18, 3339.

(9) De-La-Cuesta, J.; González, E.; Moreno, A.; Arbe, A.; Colmenero, J.; Pomposo. J.A. *Macromolecules* **2017**, 50, 6323.

(10) Sundararajan, P. *Physical Properties of Polymers Handbook*. New York: Springer **2006**

(11) He, J.; Tremblay, L.; Lacelle, S.; Zhao, Y. *Soft Matter* **2011**, *7*, 2380.

(12) Azuma, Y.; Terashima, T.; Sawamoto, M. *ACS Macro Letters* **2017**, *6*, 830.

(13) Perez-Baena, I.; Barroso-Bujans, F.; Gasser, U.; Arbe, A.; Moreno, A.J.; Colmenero, J.; Pomposo, J.A. *ACS Macro Letters* **2013**, *2*, 775.

(14) Lambert, R.; Wirotius, A. L; Taton, D. *ACS Macro Letters* **2017**, *6*, 489.

(15) Thanneeru, S.; Duay, S.S.; Jin, L.; Fu; Angeles-Boza, A.M; He, J. *ACS Macro Letters* **2017**, *6*, 652.

(16) Sanchez-Sanchez, A.; Arbe, A.; Colmenero, J.; Pomposo, J.A. *ACS Macro Letters* **2014**, 5, 439.

(17) Dunwei, W. *ACS Applied Energy Materials* **2018**, 1, 6657.

(18) Allegrezza, M.; Konkolewicz, D. *ACS Macro Letter* **2021**, 10, 433.

(19) Xu, J.; Jung, K.; Atme, A.; Shanmugam, S.; Boyer, C. *Journal of the American Chemical Society* **2014**, 136, 5508.

(20) Günther, H. *NMR Spectroscopy: Basic Principles, Concepts and Applications in Chemistry*. *Wiley-vch* **2013**.

(21) Tomovska, R.; Agirre, A.; Veloso, A.; Leiza, J.R. *Characterization Techniques for Polymeric Materials*. *Elsevier*, **2014**, 13.

(22) Ouchi, M.; Badi, N.; Lutz, J.F.; Sawamoto, M. *Nature chemistry*, **2011**, 3, 917.

(23) Sanchez-Sanchez, A.; Pomposo, J.A. *Journal of Nanomaterials*, **2015**, 2015, 1.

(24) Atkins, P.W; de Paula, J. *Physical Chemistry for the Life Sciences*. *W.H. Freeman and Company*, **2006**, Ch.6.

(25) Ulbricht, C.; Becer, C. R.; Winter, A.; Schubert U. S. *Macromolecular Rapid Communications* **2010**, 31, 827.

(26) Romero, N. A.; Nicewicz, D. A. *Chemical Review* **2016**, 116, 10075.

(27) Ferrara, S.J.; Mague, J.T.; Donahue, J.P. *Inorganic Chemistry* **2012**, 51, 215.

(28) Harlieb, M. *Macromolecular Rapid Communications* **2022**, 43, 1.